ACI MATERIALS JOURNAL TECHNICAL PAPER

Title no. 103-M11

High-Early-Strength Engineered Cementitious Composites

by Shuxin Wang and Victor C. Li

Rapid repair and retrofit of existing infrastructures demand durable high-early-strength materials that not only deliver sufficient strength within a few hours of placement but also significantly prolong the maintenance interval. This paper reports a class of newly developed polyvinyl alcohol (PVA) fiber-reinforced high-early-strength engineered cementitious composites (ECC) materials featuring extraordinary ductility. While micromechanics was applied in many aspects of the material design process, emphasis of this paper is put on the tailoring of preexisting flaw size distribution in matrix for high tensile ductility. The resulting high-early-strength ECC materials are capable of delivering a compressive strength of 21 MPa (3.0 ksi) within 4 hours after placement and retaining long-term tensile strain capacity above 2%.

Keywords: fibers; high early strength; strain.

INTRODUCTION

There is an increasing demand for durable high-early-strength or rapid-hardening concrete materials in repair and retrofit practices where minimum traffic disruption is preferred. For instance, highway transportation authorities often require the repair job to be completed in 6 to 8 hours at night so that the lane can be opened to traffic the next morning. In the past two decades, intensive experimental investigations carried out by both academic and industrial groups have led to successful formulation of concrete mixtures that can attain sufficient compressive and flexural strengths at very early ages. With various early strength gain rates, these concrete mixtures obtain high early strength by using either proprietary rapid hardening cements[1-5] or normal portland cement together with accelerating admixtures.[6-8]

Unfortunately, traditional concrete repairs often lack durability. It has been estimated that up to half of all concrete repairs fail.[9] About 3/4 of the failures are attributed to the lack of durability, with the remaining attributed to structural failures. Premature deterioration is more common in repair sites using high-early-strength concrete because many proprietary binder systems often perform unpredictably under various construction conditions. For example, reduced freezing-and-thawing resistance was found in some very high-early-strength concrete mixtures.[3] Meanwhile, early age cracking, associated with autogeneous shrinkage and/or thermal gradient under high temperature caused by rapid hydration, also exacerbates the deterioration.

Engineered cementitious composite (ECC) is a special type of high-performance fiber-reinforced cementitious composite (HPFRCC) featuring significant tensile ductility and moderate fiber volume fraction (typically 2%). The design of ECC is guided by micromechanics models, which provide quantitative links between composite mechanical behavior and the properties of the individual phases, that is, fiber, matrix, and interface.[10] Using the models, the desired high tensile ductility, which is achieved by strain-hardening and multiple-cracking, is converted to a set of constraints on individual component properties. These components, that is, the fiber, the matrix, and the interface, are then synergistically tailored to meet the constraints.

ECC is expected to be an effective repair and retrofit material due to its high ductility and tight crack width. Ductility is being gradually recognized as the most critical property for durable repair. As a repair material, ECC exhibits exceptional deformation compatibility with concrete substrate structure. The high-fracture toughness and multiple-cracking behavior enables ECC retrofit to effectively defuse and arrest unstable crack propagation initiated from the surrounding concrete or from the new/old concrete interface, and hence eliminates spalling or delamination failures, which are the common premature failure modes in repaired structures.[11-13] Unlike conventional tension-softening FRC materials, the crack width of ECC material in the strain-hardening regime is an intrinsic material property and typically below 100 μm (0.004 in.) Because the flow rate in cracked concrete scales as the third power of the crack width [14] and approaches zero when the crack width is below 100 μm (0.004 in.),[15] the transport of water through cracks in ECC cover through permeation is minimal [16] and hence prevents the corrosion of steel reinforcement underneath. In preloaded reinforced beam test under wet-dry cycles of a chloride environment, Hiraishi et al.[17] demonstrated that the steel reinforcement corrosion was significantly reduced when concrete was replaced by ECC. Furthermore, even if corrosion occurs, the strain-hardening capacity of ECC will accommodate the expansion induced by corrosion and prevent occurrence of spalling. Therefore, repair and retrofit with ECC material may significantly extend the infrastructure service life. [13,18]

Conventional ECC mixtures use Type I ordinary portland cement (OPC), which shows relatively slow strength development. As a high-strength gain rate is desired, the selection of a binder system has to take into consideration material cost, workability, practice restriction, and long-term durability. If adequate early strength can be attained, a normal portland cement-based mixture is always favored over proprietary rapid hardening cement. Even though a large number of accelerating admixtures are available on the market, very few, if any, provide a compressive strength of 2 ksi (13.8 MPa) 3 hours after placement.[5] Therefore, the selection of a binder system is highly performance orientated, that is, proprietary rapid hardening cement may be the sole choice if a stringent strength requirement has to be met. In this study, various combinations of binder systems and accelerating admixtures

ACI Materials Journal, V. 103, No. 2, March-April 2006.
MS No. 04-234 received July 21, 2004, and reviewed under Institute publication policies. Pertinent discussion including authors' closure, if any, will be published in the January-February 2007 *ACI Materials Journal* if the discussion is received by October 1, 2006.

ACI member **Shuxin Wang** *is manager of MSeals Co. Ltd., Ningbo, China. He received his BS and MS from Tsinghua University at Beijing, Beijing, China, and his PhD from the Department of Civil and Environmental Engineering at the University of Michigan, Ann Arbor, Mich. His research interests include the development of high-performance fiber-reinforced cementitious composites.*

ACI member **Victor C. Li** *is a professor of civil and environmental engineering at the University of Michigan. He is a member of ACI Committee 544, Fiber Reinforced Concrete. His research interests include micromechanics-based composite materials design and engineering, innovative structures design based on advanced materials technology, and sustainable infrastructure engineering.*

were investigated and some illustrative mixtures are presented herein.

High-early-strength ECC for rapid repair applications must meet minimum strength requirements before the structure can be returned to service. However, there is no existing standard for minimum compressive strength prior to opening to traffic. Parker and Shoemaker[6] suggested that for road patch repair 2 ksi (13.8 MPa) compressive strength was sufficient to prevent raveling, abrasion, deformation, and cracking when initially opened to traffic. The New Jersey State Department of Transportation specified target compressive and flexural strengths of 3000 and 350 psi (20.7 and 2.4 MPa), respectively, in 6 hours to the "fast-tract mix" developed in the mid-90s.[7] The California State Department of Transportation (Caltrans) requires a minimum flexural strength of 400 psi (2.8 MPa) prior to opening to traffic for full depth pavement repair.[19] This strength specification is based on pavement design and the experience of Caltrans engineers that if the slab is subjected to traffic prior to obtaining this strength, the durability and life expectancy of the repaired pavement may be jeopardized. For very high-early-strength concrete, Caltrans specifies 400 psi (2.8 MPa) flexural strength at 4 hours after placement. The FHWA *Manual of Practice: Materials and Procedures for Rapid Repair of Partial-Depth Spalls in Concrete Pavements*[20] recommends a compressive strength of 6.9 MPa (1.0 ksi) and flexural strength of 3.1 MPa (450 psi) for rapid-setting cementitious concrete. In this study, the minimum strength requirement is set to be 3 ksi (20.7 MPa) in compression and 500 psi (3.5 MPa) in flexural.

This paper presents selected results from an extensive experimental program, with emphasis on the aspect of material design. High-early-strength ECC based on rapid hardening cement and normal portland cement are reported. The experimental program comprises three phases, namely matrix design for high early strength, tailoring for tensile strain-hardening behavior, and characterization of other mechanical properties. In the first phase, the factors most pertinent to early strength gain rate, including the water-binder ratio, accelerator type, and dosage, were investigated. In the second phase, to accommodate the adverse impact on the matrix and interface micromechanical properties due to the use of high-early-strength composition, the microstructure tailoring approach is introduced to recover the tensile ductility when necessary. For those mixtures with satisfactory early strength and ductility, other mechanical properties including flexural response and Young's modulus were then measured.

RESEARCH SIGNIFICANCE

Current state-of-the-art high-early-strength cementitious materials for rapid repair, including various rapid hardening cement-based mortar and polymer mortar, are all quasi-brittle in nature. The incorporation of short reinforcing fibers, most commonly steel fiber and polypropylene fiber, does not eliminate the tension-softening behavior and low-strain capacity despite improvement in fracture energy. This paper reports a type of fiber-reinforced cementitious composite delivering very high early strength and significant tensile strain capacity. The effectiveness of micromechanics design approach is highlighted through matrix microstructure tailoring. Durability of repair or new construction using these materials is expected to be fundamentally improved due to superior deformability, limited crack width, and compatibility to existing substrates.

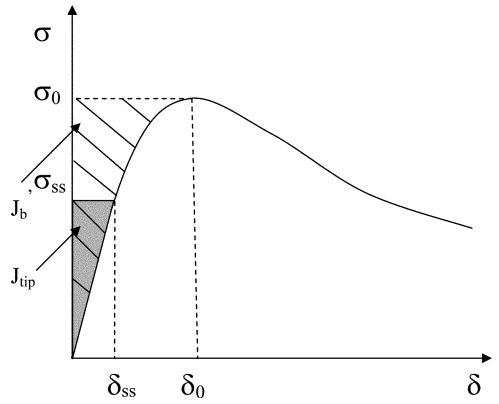

Fig. 1—Typical $\sigma(\delta)$ curve for strain-hardening composite. Hatched area represents complimentary energy J_b'. Shaded area represents crack tip toughness J_{tip}.

MATERIAL DESIGN FRAMEWORK

Strain-hardening behavior of ECC materials is obtained from careful tailoring of the constituent properties. Specifically, these properties are chosen such that steady state cracking prevails under tension. This requires the crack tip toughness J_{tip} to be less than the complementary energy J_b' calculated from the bridging stress σ versus crack opening δ curve, as illustrated in Fig. 1[21-22]

$$J_{tip} \le \sigma_0\delta_0 - \int_0^{\delta_0}\sigma(\delta)d\delta \equiv J_b' \quad (1)$$

$$J_{tip} = \frac{K_m^2}{E_m} \quad (2)$$

where σ_0 is the maximum bridging stress corresponding to the opening δ_0; E_m is the matrix elastic modulus; and K_m is the fracture toughness. Equation (1) is obtained by considering the balance of energy changes during extension of the steady state flat crack. The stress-crack opening relationship $\sigma(\delta)$, which can be viewed as the constitutive law of fiber bridging behavior, is derived by using analytic tools of fracture mechanics, micromechanics, and statistics. In particular, the energetics of tunnel crack propagation along fiber/matrix is used to quantify the debonding process and the bridging force of a fiber with given embedment length;[23] statistics are introduced to describe the random location and orientation of fibers. The random orientation of fiber also necessitates the accounting of the mechanics of interaction between an inclined fiber and the matrix crack. Another condition for

pseudo strain-hardening is that the tensile first crack strength σ_{fc} must not exceed the maximum bridging stress σ_0,

$$\sigma_{fc} < \sigma_0 \quad (3)$$

where σ_{fc} is determined by the maximum preexisting flaw size $\max[a_0]$ and the matrix fracture toughness K_m. Details of these micromechanical analyses can be found in References 23 and 24. Satisfaction of Eq. (1) and (3) is necessary to achieve ECC behavior. Otherwise, normal tensile softening FRC behavior results.

The shape of the $\sigma(\delta)$ curve, which determines the value of complementary energy J_b', is further related to a number of fiber/matrix interaction mechanisms. For hydrophilic polyvinyl alcohol (PVA) fiber, which has been used for the reinforcement of ECC materials, the fiber/matrix interaction is characterized by interfacial frictional stress τ_0, chemical bond G_d, and slip-hardening coefficient β accounting for the slip-hardening behavior during fiber pullout. In addition, snubbing coefficient f and strength reduction factor f' are introduced to account for the interaction between fiber and matrix as well as the reduction of fiber strength when pulled at an inclined angle. Besides the interfacial properties, the $\sigma(\delta)$ curve is also governed by the fiber content V_f, fiber diameter d_f, length L_f, and Young's Modulus E_f.

The aforementioned steady state cracking criteria calls for high margin between J_b' and J_{tip}, for example, the moderate matrix toughness and high complementary energy. The latter further requires judicious control of fiber geometry and interface properties such that fiber could be pulled out under sufficient resistance with limited amount of rupture. For the PVA fiber used in ECC, special surface treatment is applied to the fiber during production to reduce the excessive bond to cementitious matrix.[25] Additionally, the regular ECC mixtures contain high content of water and fly ash for controlling matrix toughness and interface properties.[26] In the design of high early strength ECC, however, fly ash content has to be reduced and a low water-cement ratio (*w/c)* is preferred for quick strength gain at early ages. The use of high-early-strength cement may also alter the interface properties, mostly unfavorable to high complementary energy.

When the margin between J_b' and J_{tip} is small, it becomes critical to control pre-existing flaw distribution in the matrix to retain high strain capacity. While Eq. (1) and (3) guarantee the occurrence of multiple-cracking, the number of the cracks that could be developed (the multiple-crack saturation level) is governed by the flaw size and their spatial distribution. Limited by the peak bridging stress, a lower bound of critical flaw size c_{mc} is set such that only those flaws larger than c_{mc} can be activated prior to reaching σ_0 and contribute to multiple cracking. Therefore, to achieve saturated multiple cracking, a sufficient number of such large flaws must exist in the matrix. In regular ECC without explicit control of flaw size distribution, low toughness matrix is often used such that the reduced c_{mc} would produce adequate margin to activate a large number of cracks. Considering the random nature of pre-existing flaws inherent to processing, one approach that can be easily adopted in practice is to introduce artificial flaws with prescribed sizes just above c_{mc} as a superimposition to the natural flaw system. A variety of particles can be used as the artificial flaws in practice, provided that the presence of these particles can cause local stress concentration in the brittle matrix under loading. A lower bound of the content of artificial flaws can be estimated from the minimum cracking spacing constrained by fiber interface properties and matrix cracking stress, while the upper bound is limited by processing and disturbance of the relatively large particles to fiber distribution. Details regarding this approach can be found in Reference 27.

Table 1—Mixture proportions

Mixture ID	Cement, kg/m^3 (lb/yd^3)	Sand, kg/m^3 (lb/yd^3)	Other aggregates, kg/m^3 (lb/yd^3)	Water, kg/m^3 (lb/yd^3)	Fine fly ash, kg/m^3 (lb/yd^3)	PVA fiber, kg/m^3 (lb/yd^3)	Admixture,* L/m^3 (fl oz/yd^3)
SC01	906† (1526)	724 (1221)	—	350 (590)	90.6 (153)	26.0 (43.8)	13.9 (359) [PT20]
SC19	863† (1455)	690 (1163)	41.4‡ (69.8)	334 (563)	86.0 (145)	26.0 (43.8)	13.3 (343) [ML330]
HP08	893§ (1506)	893 (1506)	—	292 (492)	—	26.0 (43.8)	6.3 (163) [GL3200] 25.7 (664) [NC534]
HP09	848§ (1430)	848 (1430)	54.0‖ (91.0)	278 (469)	—	26.0 (43.8)	5.9 (153) [GL3200] 24.4 (631) [NC534]
OP08	583# (983)	467 (787)	—	298 (502)	700 (1180)	26.0 (43.8)	15.0 (388) [ML330]

*PT20: accelerator and high-range water-reducing admixture containing ammonium calcium nitrate and naphthalene sulfonate salt; ML330: melamine formaldehyde sulfonate-based high-range water-reducing admixture; GL3200: polycarboxylate-based high-range water-reducing admixture; and NC534: calcium nitrate-based accelerator.

†Rapid-hardening cement (Type S-30, Korea).

‡Polypropylene (PP) beads used as artificial flaws.

§Type III cement.

‖Polystyrene (PS) beads used as artificial flaws.

#Type I ordinary portland cement.

EXPERIMENTAL PROGRAM

Extensive experiments were conducted to examine the early strength gain rate of various combinations of binder system and accelerating admixture under approximate proportion of ECC materials. In addition to Type I OPC and Type III high early strength portland cement, calcium aluminate cement, gypsum cement, and blended calcium sulfo-aluminate were also evaluated. Commercially available accelerators, which effective components include calcium chloride, calcium nitride, and ammonium calcium nitrate were used in the investigation together with a high-range water-reducing admixture that is necessary for proper fiber dispersion. A high-range water-reducing admixture, depending on chemical species, exhibits considerable influence on early strength development. High-range water-reducing admixture based on naphthalene sulfonate, melamine formaldehyde sulfonate, and polycarboxylate were tested. In addition, the influences of the water-binder ratio and sand content were also investigated.

Five illustrative mixture proportions are listed in Table 1. Mixtures SC01 and SC19 both use a rapid-hardening blended portland cement (Blaine surface area 4730 cm^2/g) with calcium sulfo-aluminate. Mixtures HP08 and HP09 both use Type III portland cement (surface area 5000 cm^2/g). Mixture OP08 is a regular ECC mixture using Type I OPC (surface area 3300 cm^2/g) and the results are presented herein for comparison. Mixtures SC01 and SC09 have same mixture proportions except that SC09 contains 4.6% by volume polypropylene (PP) particles for creating artificial flaws. These disk-shape particles with a diameter of approximately 4 mm and a thickness of approximately 2 mm have little bond to surrounding cementitious species. Similarly, Mixtures HP08 and HP09 have same mixture proportions

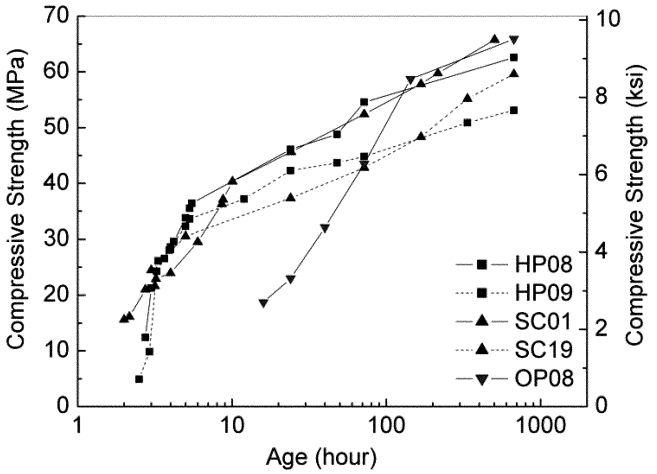

Fig. 2—Compressive strength development of rapid-hardening cement-based mixtures.

except that 5.0% by volume of polystyrene (PS) particles are introduced as artificial flaws in Mixture HP09. These PS beads have a skewed cylinder shape and sharp edges. The length of longest dimension of the PS particles is approximately 4 mm. A small amount of ultra fine fly ash [28] (surface area 8000 cm^2/g) with high reactivity is incorporated into SC01 and SC19 for rheology control. The sand used is a type of fine silica sand with size distribution from 50 to 250 μm (0.002 to 0.010 in.) and a mean size of 110 μm (0.004 in.) (8% < 53 μm, 33% < 75 μm, 77% < 100 μm, 93% < 150 μm). A special PVA fiber designed particularly for ECC applications is used at a moderate volume fraction of 2% in all mixtures. The fiber has a length of 12 mm (0.47 in.), a diameter of 39 μm (0.0015 in.), and a nominal tensile strength of 1620 MPa (235 ksi). The density of the fiber is 1300 kg/m^3 (2191 lb/yd^3). For the rapid-hardening cement-based mixtures, a powerful dispersant is sufficient to achieve rapid strength gain, and the effect of accelerator was found to be minimal regardless of its type. In SC01, a multiple purpose admixture acting as both accelerator and high-range water-reducing admixture was used, while in SC19 only melamine formaldehyde sulfonate-based high-range water-reducing admixture was used. For the Type III cement-based system, however, a combination of polycarboxylate-based high-range water-reducing admixture and calcium nitrate-based accelerator exhibits most significant accelerating effect when calcium chloride is excluded, as found in Reference 8 for high-early-strength concrete.

The ECC mixture was prepared in a Hobart-type mixer with 10L (0.35 ft^3) capacity. Solid ingredients, including cement, sand, and fly ash and particles for artificial flaws if applicable were first mixed for approximately 1 minute, then water was added and mixed for another 3 minutes. Next, a high-range water-reducing admixture was added into the mixer. Once a consistent mixture was reached, fiber was slowly added. Accelerating admixture, if used, was added before casting. The whole mixing procedure typically takes 8 to 10 minutes. The mixture was then cast into molds with moderate vibration applied. Due to small specimen dimensions, the molds were covered with plastic sheets and stored in a container with an insulation wall to reduce the loss of hydration heat. Specimens were demolded after 24 hours and then cured in air at room temperature (16 to 20 °C) before testing. For those tested before 24 hours, the specimens were demolded just before testing. The room relative humidity is 55 ± 5%.

All compressive tests use cylinder specimens 75 mm (3 in.) in diameter by 150 mm (6 in.) in height. The ends of the specimens were capped with sulfur compound. Testing began at 3 hours after casting or when adequate strength had developed. The age of the specimen was recorded as the time elapse from finish of casting to test. The mixing and casting procedure took approximately 20 to 30 minutes.

Direct uniaxial tensile test was conducted to characterize the tensile behavior of the ECC material.[26] The coupon specimen used here measures 304.8 x 76.2 x 12.7 mm (12 x 3 x 0.5 in.). Aluminum plates were glued at the ends of the coupon specimen to facilitate gripping. Tests were conducted under displacement control at a loading rate of 0.005 mm/s (0.0002 in./s). Two external linear variable displacement transducers were attached to the specimen surface with a gauge length of approximately 180 mm (7.1 in.) to measure the displacement. Young's modules was calculated from the linear elastic portion of the uniaxial stress-strain curve prior to cracking.

Flexural behavior was measured using beam specimen with dimensions of 304.8 mm (12 in.) in length by 76.2 mm (3 in.) in width by 25.4 mm (1 in.) in depth under four point bending. The span between supports was 254 mm (10 in.) and the constant moment length was 76.2 mm (3 in.). The loading rate was 0.05 mm/s (0.002 in./s), and the displacement at the loading point was recorded. It should be noted that a flexural test is not a reliable test for strain-hardening but is carried out here mainly because flexural strength are specified in some repair applications.

A single fiber pullout test was conducted to measure the fiber/matrix interfacial properties, including frictional stress τ_o, chemical bond G_d, and slip-hardening coefficient β. The specimen preparation and test method can be found in Reference 25. The data processing and calculation of the parameters follow Reference 29.

The matrix fracture toughness K_m was determined by three-point bending test compliant to ASTM E 399. The beam specimen of the matrix mixture without fiber measured 304.8 mm (12 in.) in length by 76.2 mm (3 in.) in width by 38.1 mm (1.5 in.) in depth; the loading support spanned 254.0 mm (10 in.). The notch depth-to-height ratio was 0.4.

RESULTS AND DISCUSSION

The compressive strength development of high-early-strength ECC mixtures up to 28 days is illustrated in Fig. 2, along with that of regular ECC Mixture OP08. The fast-strength gain is recorded after the first 5 hours in both the rapid-hardening cement-based mixtures and the Type III portland cement-based mixtures, in which a compressive strength of 21 MPa can be easily achieved at 3 to 4 hours after placement, sufficient for most emergency repair applications. In contrast, regular ECC OP08 develops same strength only after approximately 24 hours. Compared with rapid-hardening cement, which sets and hardens within one hour, Type III cement-based mixtures exhibit little strength at the first two hours even with the aid of an accelerator. Higher early strength can be readily achieved by further reducing water to binder ratio; however, the consequent increase in interface bond properties and matrix toughness diminishes the potential of developing multiple-cracking to an extent that only tension-softening behavior prevails.

The introduction of PP and PS beads at small volume fraction has demonstrated negligible effect on the early age compressive strength. Compared with the mixtures without

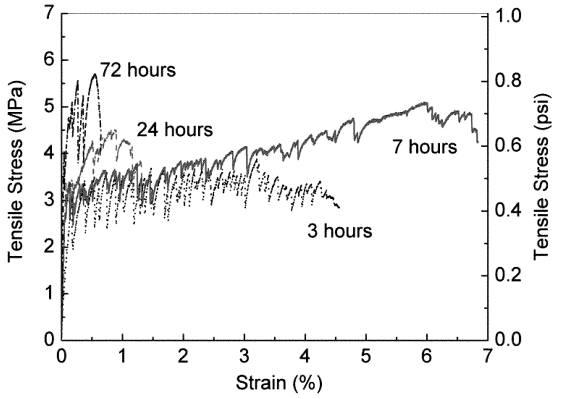

Fig. 3—Tensile behavior of rapid-hardening cement-based Mixture SC01.

artificial flaws (for example, SC01 and HP08), the corresponding mixes containing the plastic beads (for example, SC19 and HP09) show little difference in compressive strength prior to approximately 30 MPa. With maturing of the matrix, however, the weakening effect of the soft PP beads prevails due to the loss of deformation compatibility between the bead and the surrounding mortar. At 28 days, a reduction of approximately 20% in strength was observed in those mixtures with plastic beads. Nevertheless, the compressive strength of SC19 and HP09 at 28 days is considered adequate for most applications.

Figure 3 shows the tensile behavior of SC01 at different ages. A rapid decrease in strain capacity with age was observed, however, accompanied by increase of first cracking strength and ultimate tensile strength. At 3 hours after casting, the material exhibits satisfactory strain-hardening behavior with a strain capacity above 3%. The ductility is further improved at the age of 7 hours, where an ultimate strain of 6% is demonstrated. However, the strain capacity quickly decreases to about 1.0% after 24 hours and retains only 0.7% after 3 days.

The rapid decrease of strain capacity can be attributed to the continuing increase of both interfacial bond strength and matrix toughness. Figure 4 presents the age dependency of the interface properties, for example frictional stress τ_o, chemical bond G_d, and slip-hardening coefficient β, measured from single fiber pullout tests, as well as K_m determined from notched beam bending test. Despite scattering of the data, the trend clearly shows that the development of bond between fiber and matrix remains relatively slow at the first 24 hours and then accelerates considerably before finally saturating after 7 days. In particular, the gain rate of τ_o at early age is faster than G_d and β. Meanwhile, the development of K_m at early age is even faster than the interface properties, and it saturates after approximately 3 days. The different development rate may be explained by the fact that the accelerated hydration is mainly taking place among the cement species and the reactivity of fiber surface is less affected.

The evolution of micromechanical properties results in the quick change of J_b'/J_{tip} ratio that indicates the margin for strain-hardening. PVA fiber features high bond strength both frictional and chemical to hydrated cement. In addition, PVA fiber exhibits strong slip-hardening behavior during pullout. Therefore, the fiber often ruptures instead of being pulled out from the matrix. Reflecting on the micromechanical property, the premature failure of fiber leads to a diminishing complementary energy J_b'. For rapid-hardening cement-based mixture,

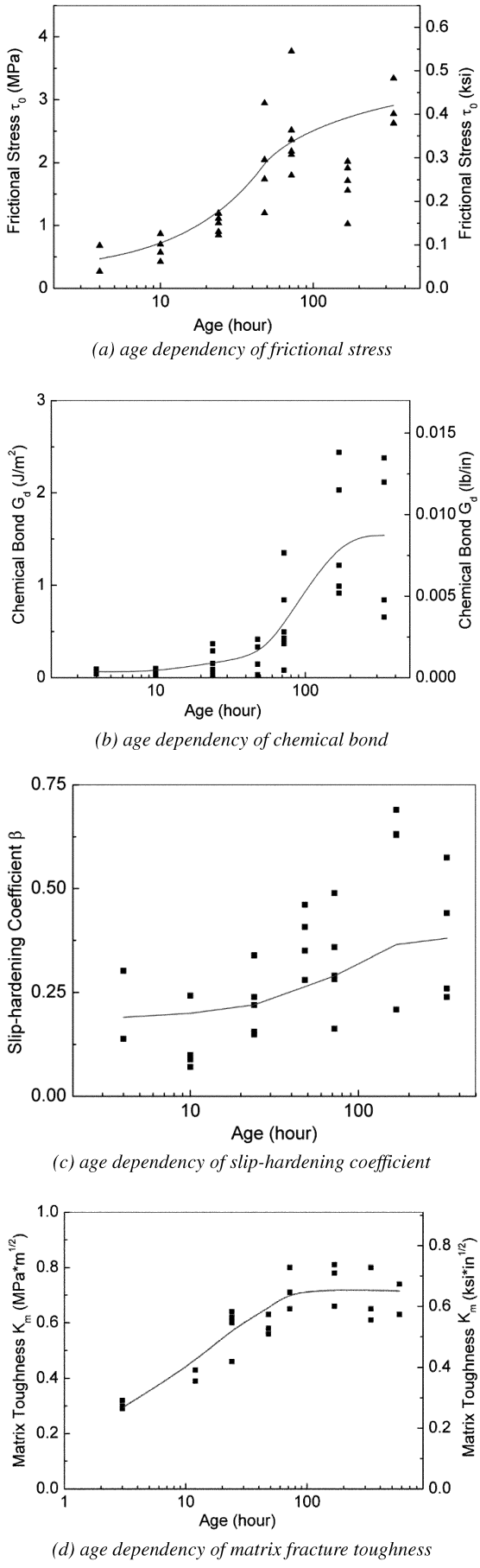

(a) age dependency of frictional stress

(b) age dependency of chemical bond

(c) age dependency of slip-hardening coefficient

(d) age dependency of matrix fracture toughness

Fig. 4—Age dependency of microchemical properties of Mixture SC01.

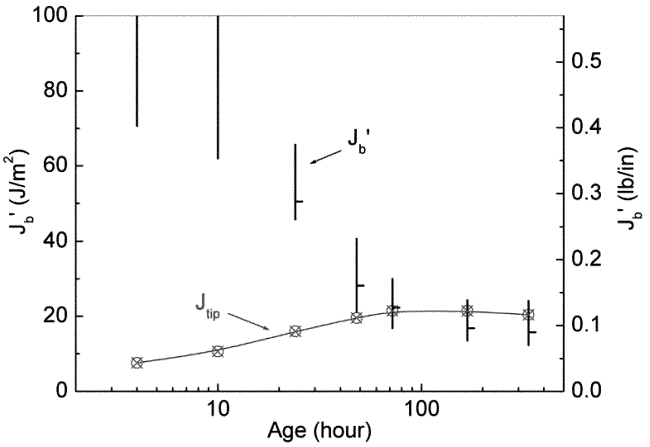

(a)

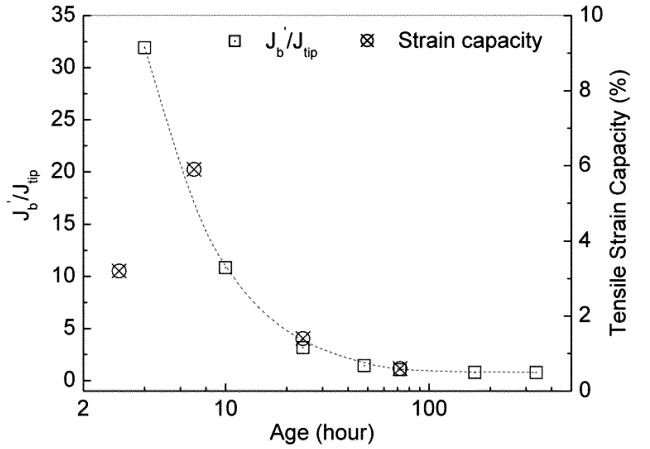

(b)

Fig. 5—Evolution of complementary J_b' *and crack tip toughness* J_{tip} *with age in Mixture SC01.*

significant increases of τ_o, G_d, and β after 24 hours cause severe fiber rupture. As illustrated in Fig. 5(a), J_b' rapidly decreases in first 48 hours, while J_{tip} increases with the maturing of the matrix. Consequently, the J_b'/J_{tip} ratio drops from approximately 15 to approximately 1 after 3 days and flattens after 7 days. Despite the simplifying assumptions made in the model that tends to underestimate J_b', the model precisely captures the nature of the deterioration of strain-hardening behavior with age. When plotting the J_b'/J_{tip} ratio and the strain capacity together against age, it is evident that both follow the same trend (Fig. 5(b)) except for the very early age at 3 hours where premature failure at the grips were encountered due to difficulty in applying epoxy glue at very early age.

For SC01, the condition for strain-hardening ($J_b'/J_{tip} > 1$) is easily satisfied at the first 24 hours, as demonstrated by the experimentally determined high strain capacities. The gap between J_b' and J_{tip} becomes rather small after 3 days. According to the criterion, strain-hardening should still occur though the diminishing margin may restrict multiple-cracking saturation. In fact, although the crack number is very limited, multiple-cracking is still observed after 3 days. Furthermore, the model indicates the possibility to achieve high strain-hardening after 7 days because J_{tip} is still within the range of J_b'.

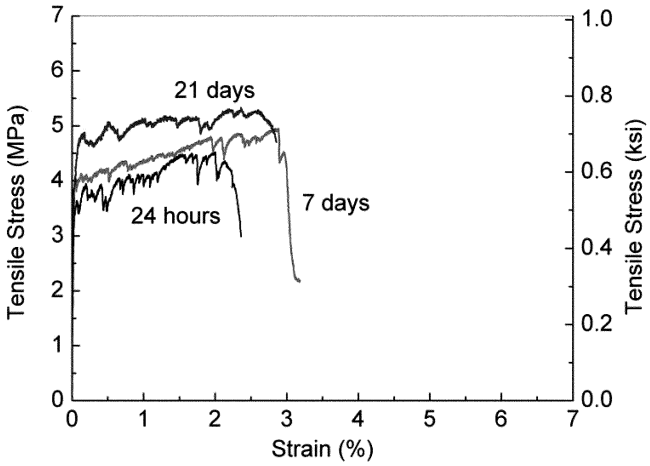

Fig. 6—Tensile behavior rapid-hardening cement-based Mixture SC19 at different ages.

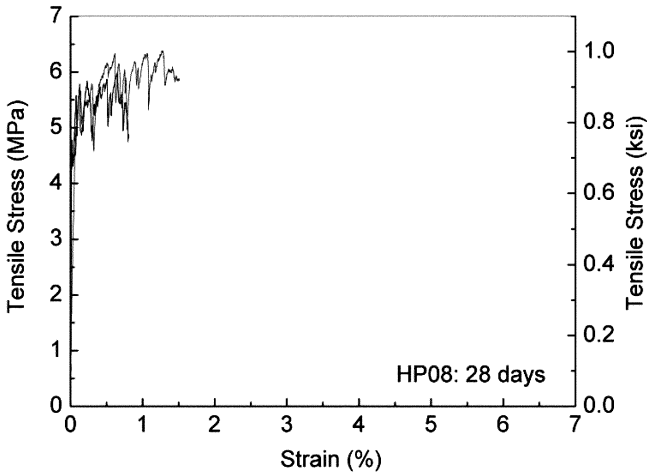

Fig. 7—Tensile behavior of Type III cement-based mixture without artificial flaws (Mixture HP08) at 28 days.

The potential of multiple-cracking is confirmed in SC19, which has same mixture proportion as SC01 except that PP beads are introduced as artificial flaws at volume fraction of 4.6%. The size of the PP beads was chosen to be comparable to the largest flaws found in section examination of the uniaxial test specimens. Figure 6 shows the tensile stress-strain curves at ages of 1, 3, and 21 days, and the strain capacity at age after 24 hours is significant increased. The strain capacity remains approximately 2.5% after 21 days, whereas the saturation of micromechanical properties has been reached at approximately 14 days (Fig. 4), suggesting that the strain capacity can be retained in the long term. Well-distributed and near-saturated multiple cracking was observed with average crack spacing of 3 to 4 mm (0.12 to 0.16 in.).

A similar trend was also seen in the Type III cement-based high-early-strength Mixture HP08, where the fine grain size of grounded portland cement along with low *w/c* necessitated for rapid strength gain cause a rapid increase in K_m and hence reduce the margin for multiple-cracking. Figure 7 shows the tensile stress-strain curve of HP08 at 28 days, where multiple-cracking behavior is evident, but strain capacity is barely above 1.0%. In contrast, with the introduction of 5.0% by volume of PS beads as artificial flaws, HP09 demonstrates strain capacity of 3.5% at 50 days, retaining

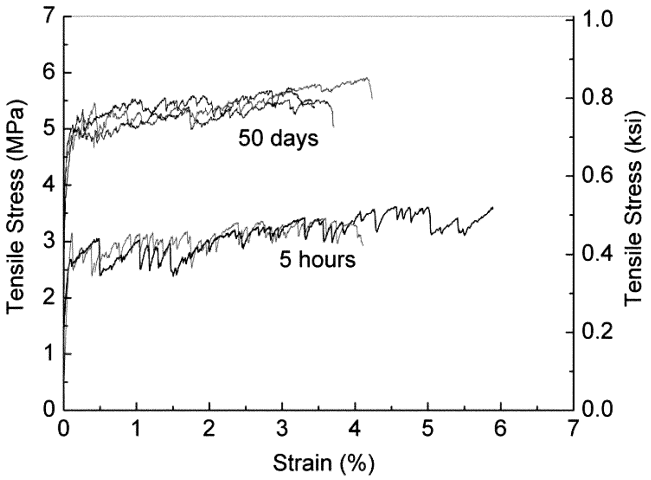

Fig. 8—Tensile behavior of Type III cement-based Mixture HP09 with artificial flaws (PS beads 5.0 vol. %) at ages of 5 hours and 50 days.

most ductility exhibited at 5 hours in spite of 100% increase of cracking strength (Fig. 8). It was also noticed that the presence of artificial flaws only slightly reduces the first cracking strength due to its well controlled size distribution. The high ductility of HP09 therefore originates from a more homogeneous defect system that imparts the potential of saturated multiple-cracking, as self-evident in comparison between the cracking patterns of HP08 and HP09 (Fig. 9). It should be mentioned that microcrack width in ECC materials remains almost constant during strain-hardening regime, and increase of strain capacity for a particular system mainly relies on increase of multiple-cracking density. For HP09, the average crack width is 65 μm (0.0026 in.), and the average crack spacing is 2.5 mm (0.1 in.).

Although the effectiveness of flaw size tailoring on improving ductility is highlighted, this approach should be viewed as supplemental to interface and matrix toughness control. Figure 10 shows typical stress-strain curves of the OPC-based ECC Mixture OP08 tested at the age of 24 hours when the 21 MPa (3.0 ksi) minimum strength criterion is reached and at the age of 90 days when hydration has been stabilized. In both cases, strain capacity about 2.5% is recorded, even though the flaw system is not deliberately tailored. The selection of binder composition, water-binder ratio, sand content, and fiber properties in OP08 has ensured relatively large margin between J_b' and J_{tip} such that sufficient natural flaws can be activated for multiple cracking. In the design of high-early-strength ECC, these micromechanics criteria were also followed in the selection of mixture proportion, which enables the further tailoring of flaw size distribution.

Figure 11 illustrates the deflection-hardening behavior of SC19, HP09, and OP08 at different ages. The cracking strength and ultimate flexural strength of SC09 are 4.5 MPa (0.65 ksi) and 6.7 MPa (0.97 ksi), respectively, at 3 hours after placement, which are considerably higher than conventional high early strength repair mortar. At later age, the flexural strength stabilizes at about 15 MPa (2.17 ksi). Compared with SC09, flexural ductility of HP09 is noticeably higher at the same age, while similar ultimate flexural strength was observed. At 4 hours after placement, the material delivers 10 MPa (1.45 ksi) flexural strength. It was noticed that the presence of artificial flaws had a less significant effect on the flexural behavior than on the uniaxial tensile behavior. For

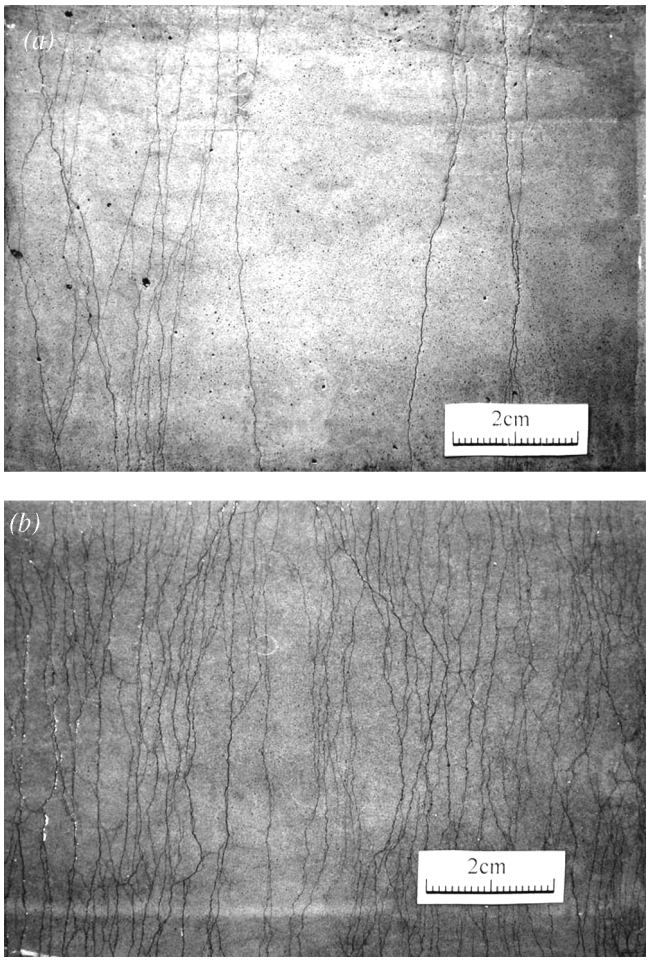

Fig. 9—Cracking patterns of Type III cement-based mixtures: (a) unsaturated multiple-cracking in Mixture HP08 at 28 days; and (b) near-saturated multiple-cracking in Mixture HP09 with artificial flaws at 50 days.

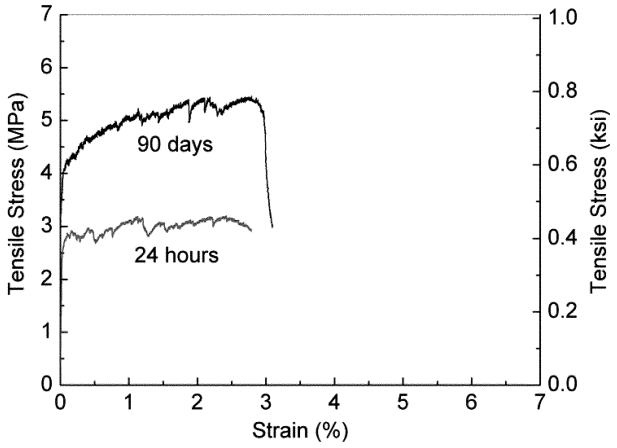

Fig. 10—Typical stress-strain curves of OPC-based regular ECC Mixture OP08 at 24 hours and 90 days.

instance, the bending response of OPC-based OP08 without artificial flaws demonstrated higher ductility, though OP08 showed less tensile strain capacity in uniaxial tension tests compared with HP09. One plausible explanation is that the cracking initiation effect of the artificial flaws, which is dominant under uniaxial tension, is masked by the stress gradient effect (cracks propagate from tensile into compression

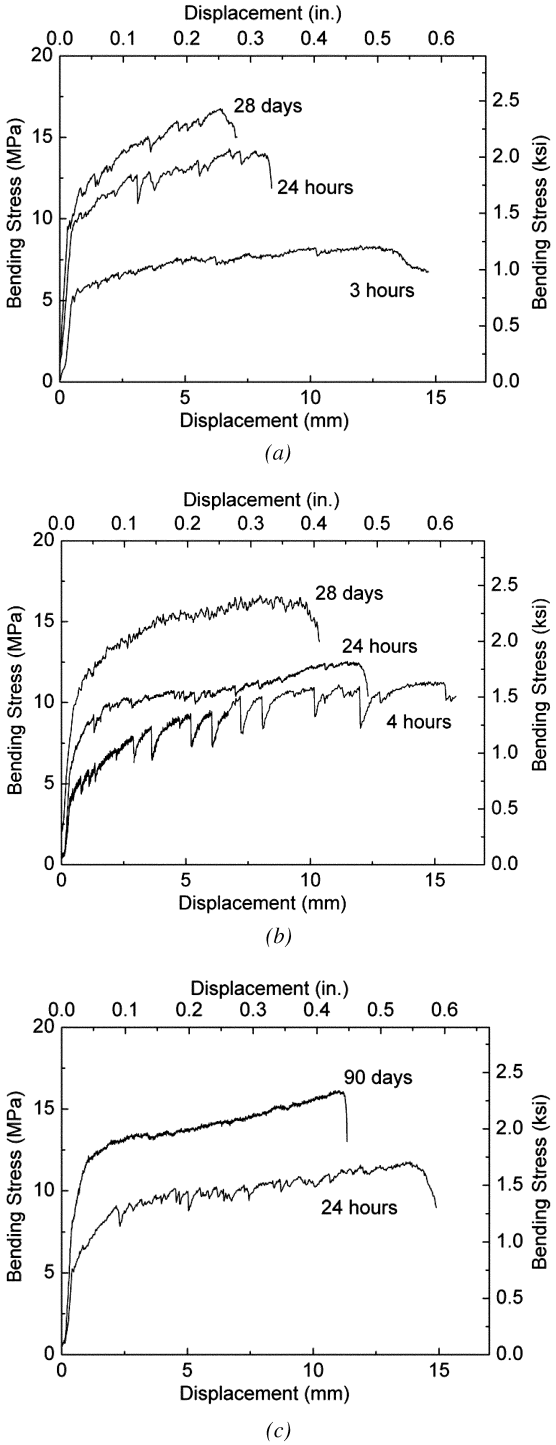

Fig. 11—Typical bending behaviors of: (a) Mixture SC19; (b) Mixture HP09; and (c) Mixture OP08 at different ages.

zone of beam) under flexural bending that stabilizes crack propagation and allows more cracks to be developed. As a result, a composite hardly showing strain-hardening under uniaxial tension may exhibit unambiguous flexural deflection-hardening as observed in many FRC materials. This behavior, however, is dependent on beam height.

CONCLUSIONS

High-early-strength ECC materials based on various binder systems were developed under the guidance of micromechanical models. Table 2 summarizes the typical mechanical properties of two exemplary ECC mixtures based on rapid-hardening cement and Type III portland cement respectively, along with that of the regular ECC mixture which uses ordinary portland cement for comparison. In particular, the following conclusions can be drawn:

Table 2—Mechanical properties of examples

Mixture ID	SC19	HP09	OP08
Compressive strength, MPa (ksi)	24 (3.5) at 3 h 37 (5.4) at 24 h 60 (8.7) at 28 days	26 (3.8) at 4 h 42 (6.1) at 24 h 53 (7.7) at 28 days	18 (2.6) at 16 h 24 (3.5) at 24 h 65 (9.4) at 28 days
Flexural strength, MPa (ksi)	7.0 (1.0) at 3 h 14 (2.0) at 24 h 16 (2.3) at 28 days	10 (1.4) at 4 h 12 (1.7) at 24 h 16 (2.3) at 28 days	11 (1.6) at 24 h 15 (2.2) at 28 days
Tensile strength, MPa (ksi)	3.5 (0.5) at 3 h 3.5 (0.5) at 24 h 5.2 (0.8) at 28 days	3.5 (0.5) at 3 h 3.2 (0.5) at 5 h 5.5 (0.8) at 28 days	3.5 (0.5) at 3 h 3.0 (0.4) at 24 h 5.5 (0.8) at 28 days
Tensile strain capacity, %	>2.0	>3.0	>3.0
Young's modulus, GPa (ksi)	20.8 (3014) at 28 days	22.8 (3304) at 28 days	21.0 (3043) at 28 days

1. Proprietary rapid-hardening cement needs to be used when stringent high early strength is required, for example, 21 MPa (3.0 ksi) within 3 hours. The exemplary mixture delivers 24 MPa (3.5 ksi) compressive strength at 3 hours and retains tensile strain capacity above 2.0% in the long term;

2. The Type III portland cement-based mixture containing a polycarboxylate-based high-range water-reducing admixture and calcium nitrate-based accelerator is capable of attaining 21 MPa (3.0 ksi) at 4 hours and retain strain capacity 3.5% at 50 days;

3. The development of interface frictional stress, chemical bond and slip-hardening coefficient of PVA fiber in rapid-hardening cement-based mixture remains slow at first 24 hours, then accelerates and finally stabilizes after 14 days, while the matrix fracture toughness evolves at a faster pace and saturates after about 3 days. Micromechanics model reveals that the quick deterioration in strain capacity can be attributed to rapid drop of complementary energy and continuous rise of crack tip toughness;

4. In particular, the matrix microstructure tailoring flaw-size distribution control is necessary to promote multiple-cracking in high-early-strength ECC. Introduction of artificial flaws with prescribed size distribution has been demonstrated to be an effective approach to retain high strain capacity at late age. The presence of a small volume fraction (for example, 5%) of graded plastic particles with weak bond-to-cement hydrates results in nearly saturated multiple cracking; and

5. Although the bending response benefits less from the artificial flaw tailoring approach, high-early-strength ECC materials in general show significant deflection-hardening behavior. The flexural strength reaches 10 MPa (1.4 ksi) in 4 hours and 16 MPa (2.3 ksi) at a late age.

ACKNOWLEDGMENTS

The authors would like to thank Wonha Construction Co. Ltd., Korea, and the Michigan Department of Transportation for supporting this research.

REFERENCES

1. Seehra, S. S.; Gupta, S.; and Kumar, S., "Rapid Setting Magnesium Phosphate Cement for Quick Repair of Concrete Pavements—Characterization and Durability Aspects," *Cement and Concrete Research*, V. 23, No. 2, 1993, pp. 254-266.

2. Knofel, D., and Wang, J. F., "Properties of Three Newly Developed Quick

Cements," *Cement and Concrete Research*, V. 24, No. 5, 1994, pp. 801-812.

3. Whiting, D., and Nagi, M., "Strength and Durability of Rapid Highway Repair Concretes," *Concrete International*, V. 16, No. 9, Sept. 1994, pp. 36-41.

4. Sprinkel, M. M., "Very-Early-Strength Latex-Modified Concrete Overlay," *Report No.* VTRC99-TAR3, Virginia Department of Transportation, Richmond, Va., 1998, 11 pp.

5. Baraguru, P. D., and Bhatt, D., "Rapid Hardening Concrete," *Report* No. FHWA NJ 2001-3, New Jersey Department of Transportation, Trenton, N.J., 2000, 22 pp.

6. Parker, F., and Shoemaker, M. L., "PCC Pavement Patching Materials and Procedures," *Journal of Materials in Civil Engineering*, ASCE, V. 3, No. 1, 1991, pp. 29-47.

7. Kurtz, S.; Balaguru, P.; Consolazio, G.; and Maher, A., "Fast Track Concrete for Construction Repair," *Report No.* FHWA 2001-015, New Jersey Department of Transportation, Trenton, N.J., 1997, 67 pp.

8. Anderson, J.; Daczko, J.; and Luciano, J., "Producing and Evaluating Portland Cement-Based Rapid Strength Concrete," *Concrete International*, V. 25, No. 8, Aug. 2003, pp. 77-82.

9. Mather, B., and Warner, J., "Why do Concrete Repairs Fail," interview held at University of Wisconsin, Department of Engineering Professional Development, Wis., <http://aec.engr.wisc.edu/resources/rsrc07.html>, accessed Dec. 2004.

10. Li, V. C., "Engineered Cementitious Composites—Tailored Composites through Micromechanical Modeling," *Fiber Reinforced Concrete: Present and the Future*, N. Banthia, A. Bentur, and A. Mufti, eds., Canadian Society for Civil Engineering, Montreal, Quebec, Canada, 1998, pp. 64-97.

11. Lim, Y. M., and Li, V. C., "Durable Repair of Aged Infrastructures Using Trapping Mechanism of Engineered Cementitious Composites," *Journal of Cement and Concrete Composites*, V. 19, No. 4, 1997, pp. 373-385.

12. Li, V. C.; Horii, H.; Kabele, P.; Kanda, T.; and Lim, Y. M., "Repair and Retrofit with Engineered Cementitious Composites," *Engineering Fracture Mechanics*, V. 65, 2000, pp. 317-334.

13. Li, V. C., "High Performance Fiber Reinforced Cementitious Composites as Durable Material for Concrete Structure Repair," *International Journal for Restoration of Buildings and Monuments*, V. 10, No. 2, 2004, pp. 163-180.

14. Tsukamoto, M., "Tightness of Fiber Concrete," *Darmstadt Concrete*, V. 5, 1990, pp. 215-225.

15. Wang, K.; Jansen, D. C.; Shah, S.; and Karr, A. F., "Permeability Study of Cracked Concrete," *Cement and Concrete Research*, V. 27, No. 3, 1997, pp. 381-393.

16. Lepech, M., and Li, V. C., "Water Permeability of Cracked Cementitious Composites," Proceedings of ICF11, *Paper 4539*, Turin, Italy, Mar. 2005. (CD-ROM)

17. Hiraishi, Y.; Honma, T.; Hakoyama, M.; and Miyazato, S., "Steel Corrosion at Bending Cracks in Ductile Fiber Reinforced Cementitious Composites," *Proceedings of the JCI Symposium on Ductile Fiber Reinforced Cementitious Composites (DFRCC)*, Tokyo, Japan, 2003. (in Japanese)

18. Li, V. C., and Lepech, M., "Crack Resistant Concrete Material for Transportation Construction," Transportation Research Board 83rd Annual Meeting, Washington, D.C., Compendium of Papers, *Paper* 04-4680, 2004. (CD-ROM)

19. "Paving Repair Finds a Four-Hour Champion," *Concrete Construction*, V. 46, No. 12, 2001, pp. 69-70.

20. Federal Highway Administration (FHWA), *Manual of Practice: Materials and Procedures for Rapid Repair of Partial-Depth Spalls in Concrete Pavements*, 1999, 135 pp.

21. Marshall, D. B., and Cox, B. N., "A J-Integral Method for Calculating Steady-State Matrix Cracking Stresses in Composites," *Mechanics of Materials,* No. 8, 1988, pp. 127-133.

22. Li, V. C., and Leung, C. K. Y., "Theory of Steady State and Multiple Cracking of Random Discontinuous Fiber Reinforced Brittle Matrix Composites," *Journal of Engineering Mechanics*, ASCE, V. 118, No. 11, 1992, pp. 2246-2264.

23. Lin, Z.; Kanda, T.; and Li, V. C., "On Interface Property Characterization and Performance of Fiber-Reinforced Cementitious Composites," *Journal of Concrete Science and Engineering*, RILEM, No. 1, 1999, pp. 173-184.

24. Li, V. C., "Post-Crack Scaling Relations for Fiber-Reinforced Cementitious Composites," *Journal of Materials in Civil Engineering*, ASCE, V. 4, No. 1, 1992, pp. 41-57.

25. Li, V. C.; Wu, C.; Wang, S.; Ogawa, A.; and Saito, T., "Interface Tailoring for Strain-Hardening Polyvinyl Alcohol-Engineered Cementitious Composite (PVA-ECC)," *ACI Materials Journal*, V. 99, No. 5, Sept.-Oct. 2002, pp. 463-472.

26. Li, V. C.; Wang, S.; and Wu, C., "Tensile Strain-Hardening Behavior of PVA-ECC," *ACI Materials Journals*, V. 98, No. 6, Nov.-Dec. 2001, pp. 483-492.

27. Wang, S., and Li, V. C., "Tailoring of Pre-Existing Flaws in ECC Matrix for Saturated Strain Hardening," *Proceedings of FRAMCOS-5*, Vail, Colo., Apr. 2004, pp. 1005-1012.

28. Obla, K. H.; Hill, R. L.; Thomas, M. D. A.; Shashiprakash, S. G.; and Perebatova, O., "Properties of Concrete Containing Ultra-Fine Fly Ash," *ACI Materials Journal*, V. 100, No. 5, Sept.-Oct. 2003, pp. 426-433.

29. Redon, C.; Li, V. C.; Wu, C.; Hoshiro, H.; Saito, T.; and Ogawa, A., "Measuring and Modifying Interface Properties of PVA Fibers in ECC Matrix," *Journal Materials in Civil Engineering*, ASCE, V. 13, No. 6, 2001, pp. 399-406.